

# The effects of $\text{SiO}_2@Y_2O_3S:Eu^{3+}$ phosphor on the optic characteristics of white light-emitting diodes

Van Liem Bui<sup>1</sup>, Phan Xuan Le<sup>2</sup>

<sup>1</sup>Faculty of Fundamental Science, Industrial University of Ho Chi Minh City, Ho Chi Minh City, Vietnam

<sup>2</sup>Faculty of Mechanical-Electrical and Computer Engineering, School of Engineering and Technology, Van Lang University, Ho Chi Minh City, Vietnam

## Article Info

### Article history:

Received Oct 29, 2021

Revised Jun 5, 2022

Accepted Jun 19, 2022

### Keywords:

$\text{Ca}_2\text{Al}_3\text{O}_6\text{F:Eu}^{2+}$

Color uniformity

Luminous flux

Mie-scattering theory

White light-emitting diodes

## ABSTRACT

The study investigated the effectiveness of coating silica nanoparticles ( $\text{SiO}_2$ ) and resin-silica nanocomposites poly methyl methacrylate (PMMA)-silica over the surface of  $Y_2O_3S:Eu^{3+}$  red phosphors. The purpose of this surface coating is to enhance the optical properties, including the photoluminescence (PL) and long-term stability, of  $Y_2O_3S:Eu^{3+}$ . Two methods used to coat the phosphor with 5-nm silica nanoparticles are dip-coating and sol-gel (Stöber) methods.  $\text{SiO}_2$  nanoparticles were formed via hydrolysis and condensation reactions, while radical polymerization was performed to fabricate the poly (1-vinyl-2-pyrrolidone). The  $Y_2O_3S:Eu^{3+}$  surface coating of PMMA-silica composite was performed via two reactions. One is the reaction of  $\text{SiO}_2$  nanoparticles with methyl methacrylate (MMA) monomer, and the other is MMA-tetraethyl orthosilicate (TEOS) reaction. The results showed that by using the latter method,  $Y_2O_3S:Eu^{3+}$  yielded better PL and long-term stability. Additionally, surface coating with the PMMA- $\text{SiO}_2$  nanocomposite using the second technique resulted in 5% enhancement in PL and stabilized the cathode luminescence (CL) intensity of  $Y_2O_3S:Eu^{3+}$ , compared to those properties of uncoated  $Y_2O_3S:Eu^{3+}$  phosphor particles.

This is an open access article under the [CC BY-SA](https://creativecommons.org/licenses/by-sa/4.0/) license.



## Corresponding Author:

Phan Xuan Le

Faculty of Mechanical-Electrical and Computer Engineering, School of Engineering and Technology

Van Lang University, Ho Chi Minh City, Vietnam

Email: le.px@vlu.edu.vn

## 1. INTRODUCTION

The white light-emitting diode (WLED) has emerged as a potential conserve energy device that can replace the traditional incandescent and halogen light bulbs [1], [2]. In addition to that, these traditional lighting sources generate lots of heat, which probably causes danger and discomfort to the users. Compared to these conventional light sources, the LED has been reported to consume less energy to run, has longer lifespan, lower the cost of maintenance, and even increase the comfort and safety for users [3]-[5]. Thus, LED development and production have been intensively and continuously investigated and carried out. In the LED package, phosphor is considered as an indispensable component; and the phosphor mostly used in LED fabrication is the YAG ( $Y_3Al_5O_{12}:Ce$ ) yellow phosphor. The commercial WLED is comprised of a LED chip emits blue lighting and YAG phosphor emits yellow lighting, yet the color rendering indicator (CRI) of this WLED is poor (approximately 60-70) as there are only two color components in its generated white light. Then, the three-color principle was applied to white LED production [6]-[8]. In particularly, it is possible to fabricate a WLED by combining green, red and blue-emitting components in the package. Previous studies reported the combination of green, red and blue LED chips in one package, or precoating the UV LED with

three phosphors emitting those colors, or spread the red and green phosphors over the blue LED chip. The three phosphors that have been generally used for the WLED with a near-UV InGaN-LED chip are the red  $Y_2O_2S:Eu^{3+}$ , green ZnS and blue  $BaMgAl_{10}O_{17}:Eu^{2+}$  phosphors. However, to achieved a better CRI using this three-phosphor combination, it requires a large proportion of  $Y_2O_2S:Eu^{3+}$  red phosphor due to the lower red-phosphor photoluminescence intensity, by comparison with the blue and green-phosphor one [9]. Additionally, the red  $Y_2O_2S:Eu^{3+}$  has an unstable performance under the near-UV radiation. As a result, it is essential to address the problems red phosphor  $Y_2O_2S:Eu^{3+}$  have been facing for the further development of WLEDs. To reach this goal, various researches have been conducted [10]-[12]. Among that, the doping compound of alkaline earth sulfides and rare earth ion activators have been introduced to be better than the red phosphor  $Y_2O_2S:Eu^{3+}$ . Nevertheless, they are prone to instability under moisture or other air components. Besides, the phosphor's surface coating has been studied with an aim of solving the mentioned problems of  $Y_2O_2S:Eu^{3+}$  red phosphors to enhance their performances, when being applied in LED productions. In particular, the oxide-coating was proposed to phosphor particles, for instances, silica,  $Y_2O_3$ , ZnO, MgO, and organic polymer-coatings, to be compatible with specifications of WLED devices [13]-[15]. The surface coating can strengthen the phosphor-glass substrate adhesion, enhance the stability of phosphor materials under the air condition, and avoid the radiation damaging the phosphors.

To prevent the significant decrease in PL when using the coated phosphor materials, the coating layer must be transparent, and the amount of oxides must be carefully calculated and uniformly spread over the surface of each phosphor particle. A homogenous coating layer also improves the stability of the phosphor. It is noted that a uniform coating layer can be achieved when using the small particles whose sizes are even by comparison with each other. Therefore, the preparation of disaggregated monodisperse nanoparticles is crucial to the phosphor-coating-layer fabrication. In this article, we use silica ( $SiO_2$ ) nanoparticles and poly (meth-ylmethacrylate) (PMMA)-silica nanocomposite for covering film over the outside of red-color  $Y_2O_2S:Eu^{3+}$  phosphor in order to achieved the enhancement in both intensity and stability of photoluminescence. To coat the red phosphor particle with  $SiO_2$  nanoparticles, we use two different processes of dip-covering ( $P_1$ ) and sol-gel ( $P_2$ ). The PMMA-silica (PMMA- $SiO_2$ ) nanocomposite phosphor-coating is also fabricated via two processes. The first one is reacting the mixture of  $SiO_2$  nanoparticles, methyl methacrylate (MMA) monomer, initiator, and phosphor ( $P_3$ ), while the second one utilizes simultaneously reacting mixture containing MMA monomer along with tetraethyl orthosilicate (TEOS) ( $P_4$ ). The preparation of the phosphor for surface coating layer, the simulation of the WLED with the coated phosphors, and the scattering analysis of the phosphor are presented in the next part, section 2. The achieved results in terms of the coated phosphors' morphology, PL and stability are reported and discussed in section 3; and section 4 is the outcome in which the study process and achievements are summarized.

## 2. PREPARATION AND SIMULATION

### 2.1. Materials and procedures

To fabricate  $SiO_2$  nanoparticles for the phosphor coating, the concentrations of the substances participating in reaction processes, including TEOS,  $H_2O$ , the catalyst (ammonium hydroxide), the heat along with the atmosphere required for the reactions are varied to control the size of  $SiO_2$  nanoparticles. In addition to that, changing the heat and atmosphere during the reaction process helps in the prevention of agglomeration of silica nanoparticles with sizes lower than 25 nm. The reaction of silica nanoparticles with other substances was carried out for an hour.

We used a JEM-3010 transmission electron microscope (TEM) for the task of assessing the morphologies in the  $SiO_2$  nanoparticles and the uncoated and coated  $Y_2O_2S:Eu^{3+}$  red phosphors [16]-[18]. The images of each sample were then taken from 10 different specimens. A software for analyzing image (Korea) was applied to analyze and compute 10 obtained TEM images to result in the average particle size. The silica-coated and PMMA-silica nanocomposite coated phosphors were investigated with FTIR (USA) and energy dispersive spectroscopy (England). A detector of monochromator and photomultiplier (Korea) was used to measure the PL of the phosphor. The measurement was performed at the temperature of 30 °C under a 254-nm wave excited from a xenon lamp (150 W), and the 1-nm emission slit width was used to record the exhibited PL spectra. For each phosphor, there were PL examinations conducted on its 5 specimens, all of which were double-tested and the average results were recorded. The lasting steadiness of the phosphors along the irradiation process or degraded period was tested via the cathodeluminescence (CL) measurement which was performed under an electron beamline bombardment of 10 kilovolts as well as current strength measured at 45  $\mu A/cm^2$  within 30 minutes. Besides, for testing the endurance and resistance of the coated phosphor against the heat and moisture, the samples were put into a container with heat-controlled moisture (Korea) and aged under the condition of 100 °C and 80% fairly moisture, subsequently, the shifts in their PL strength within the degraded period were examined.

## 2.2. Simulation

The simulation of double-film phosphor configuration WLEDs was made with the LightTools 8.1.0 application, supported by using the scattering analysis of phosphor particles based on Mie-theory, see Figure 1. These two media also applied to investigate the effects of  $\text{SiO}_2@Y_2O_2S:Eu^{3+}$  phosphor on the optic characteristics of WLEDs with low and high (5600 K and 6600 K) color correlated temperatures (CCTs), as shown in Figures 1(a) and (b). Figure 1(c) presented the details of the WLED model used in the study. According to Figure 1 (d), the in-cup phosphor structure of the WLED package is the dual-film layout, in which the phosphor  $YAG:Ce^{3+}$  emits yellow light was put below the red phosphor layer of  $\text{SiO}_2@Y_2O_2S:Eu^{3+}$ , and both of them are located above the blue LED chips.

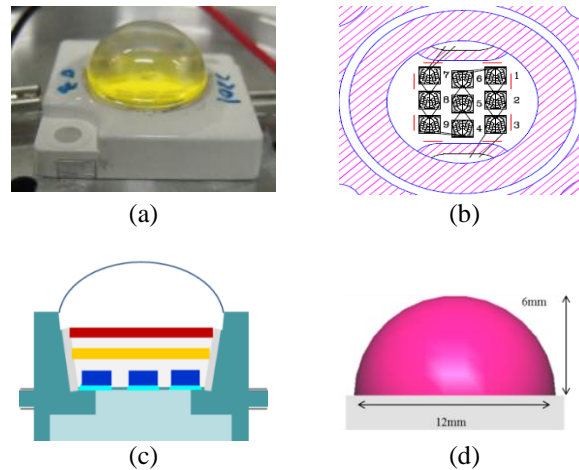


Figure 1. Picture depicting a WLED device's configuration; (a) real WLED device, (b) binding graph, (c) pc-WLED device's model, and (d) WLED modeling utilizing LightTools application

## 2.3. Scattering computation

The scattering calculation was carried out using the hypothesis of Mie-scattering [19], [20]. Accordingly, the computation of the diffusing factor  $\mu_{sca}(\lambda)$ , anisotropy factor  $g(\lambda)$ , as well as decreased diffusing factor  $\delta_{sca}(\lambda)$  are expressed via:

$$\mu_{sca} = \int N(r)C_{sca}(\lambda, r)dr \quad (1)$$

$$g(\lambda) = 2\pi \int_{-1}^1 p(\theta, \lambda, r)f(r)\cos\theta d\cos\theta dr \quad (2)$$

$$\delta_{sca} = \mu_{sca}(1 - g) \quad (3)$$

In which,

$N(r)$ : the diffusive particles' distribution density ( $\text{mm}^3$ )

$C_{sca}$ : the diffusing cross sections ( $\text{mm}^2$ )

$p(\theta, \lambda, r)$ : phase function

$\lambda$ : illuminating wavelength (nm)

$r$ : diffusive granules' radius ( $\mu\text{m}$ )

$\theta$ : diffusing angle ( $^\circ\text{C}$ )

The Stöber method was applied to synthesize the nearly mono-disperse and spherical  $\text{SiO}_2$  nanoparticles [21], [22]. As previously established, altering the dissolvent (methanol or ethanol), quantity for participating ingredients in the reacting process ( $\text{H}_2\text{O}$ , TEOS), as well as ammonium hydroxide ( $\text{NH}_4\text{OH}$ ) catalyst resulted in  $\text{SiO}_2$ -nanoparticle production with particle sizes ranging from 10 to 450 nm. It is reported that as the concentrations of TEOS and  $\text{NH}_4\text{OH}$  decreased, and the content of water increased, the size of particles showed a decline [23], [24]. Accordingly, the solvents utilized for synthesizing the nearly mono-disperse silica nanoparticles (particle size ranging from 50 nm to 450 nm) and the silica nanoparticles (particle size from 10 nm to 50 nm) were ethanol and methanol, respectively. As the nuclei size in different solvents is not the same as each other, there are variation in silica nanoparticles' size with the corresponding

solvents. It is reported that the formation of nearly monodisperse and spherical nanoparticles was observed with the particle size above 25 nm. Yet, the particle aggregation also occurred when the size of SiO<sub>2</sub> nanoparticles was smaller than 25 nm. Therefore, it is important to get the SiO<sub>2</sub> particle size decreased to avoid the aggregate formation, which can be obtained via the change of the medium and temperature condition in the reactions.

The change in particle size of silica nanoparticles was observed with various reaction temperature, as demonstrated in Figure 2. It is noted that the concentrations of reactants and the catalyst were fixed (0.28 mol TEOS, 10 mol water, 2 mol NH<sub>4</sub>OH), while the used solvent was methanol (1 L). The result showed that when the reaction temperature increased, the particle size tended to go down and then became constant. At 30 °C reaction temperature, the particle size of nearly monodisperse silica nanoparticles was 50 nm, and started to decrease when the temperature increased. At or above 80 °C, the obtained particle size of nearly monodisperse silica nanoparticles was 10 nm. Besides, when the particle size grew over 30 nm, it formed the nearly monodisperse and spherical nanoparticles. Meanwhile, the aggregate formation was also observed with primary silica nanoparticles having the particle size smaller than 20 nm. This can be attributed to the aggregate features of the particles. Particularly, the formation of smaller particles leads to the higher number of produced particles. In addition, because the outer tension of small particles is larger than large particles, they are more inclined to agglomerate in order to stabilize their surface. Hence, the aggregation forming the network structure can be observed in the case of primary silica particles with smaller size (below 20 nm), while it did not occur in the formation process of spherical particles with larger size (30 nm).

The size reduction of silica nanoparticles also occurred with the increase in water concentration, specifically, at 30 °C reaction temperature, increasing the water amount could decrease the silica nanoparticle size to 10 nm from its prepared size of 50 nm. Moreover, when increasing the water concentration, and the reaction temperature to 80 °C simultaneously, the particle size was further lower, as presented in Figure 3. However, the aggregate formation still occurred as the particle size was below 20 nm. Therefore, it can be said that, heightening the reaction temperature can get SiO<sub>2</sub>-nanoparticle size further reduced but cannot prevent the formation of particle aggregation.

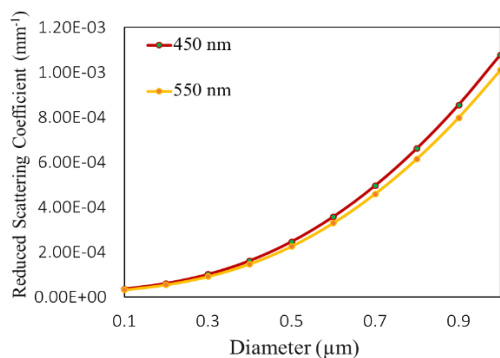


Figure 2. Reduced scattering coefficient in granules of SiO<sub>2</sub> under 450 nm as well as 550 nm

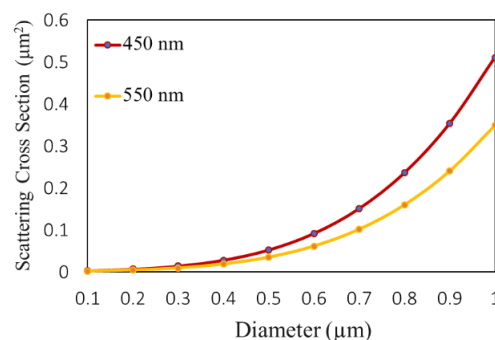


Figure 3. The diffusing cross section in granules of SiO<sub>2</sub> under 450 nm as well as 550 nm

### 3. RESULTS AND DISCUSSION

We added vinyl pyrrolidone monomer (VPM) into the mixture of reactants to prevent the aggregation when fabricating the nearly mono-disperse SiO<sub>2</sub> nanoparticle with the size smaller than 20 nm. Adding VPM in conjunction with a suitable amount of azobisisobutyronitrile (AIBN) initiator can simultaneously activate the hydrolysis and condensation reactions, resulting in silica nanoparticles, as well as the fundamental chemical process, resulting in polyvinylpyrrolidone (PVP). The amounts of VPM and AIBN initiator in the mixture of reactants were fixed at 0.2 mol and 0.5 wt% of VP monomer, respectively. The changes of silica nanoparticle size with different reaction temperatures were displayed in Figure 4. As can be seen, the size of silica nanoparticles decreased with the presence of VPM in the mixture, at all values of the reaction temperature. Moreover, with VP monomer, the primary silica nanoparticles with the size about 10 nm did not form any aggregate, as shown in Figure 5. Nevertheless, when the size of silica nanoparticles decreased to about 5 nm, the aggregate formation still occurred.

To eliminate the formation of aggregate with the primary silica nanoparticles equal or smaller than 5 nm, we increased the concentration of VP monomer to 0.4 mol. It is noted that, the concentrations of the others components in the reaction mixture remained the same. The results demonstrated in Figure 6 met our

expectations. The silica nanoparticles were formed without aggregate formation as their size was decreased from 10 nm to 5 nm. Additionally, when continuing reducing the particle size to approximately 3 nm, the aggregate formation did not occur. From these results, it is obvious that the VP monomer can help to prevent the aggregation of small particle (less than 20 nm) when it is added into the reaction mixture with an appropriate amount. Besides, due to the property of PVP, being soluble in water and methanol, using centrifugation can easily separate the formed silica nanoparticles from the resulting solution. In short, mixing a suitable proportion of VP monomer with the reaction mixture can fabricate the nearly monodisperse silica nanoparticles with particle size below 25 nm without forming particle aggregation. Finally, the silica nanoparticles with the size reduced to 5 nm were selected producing the phosphor surface coating in this study.

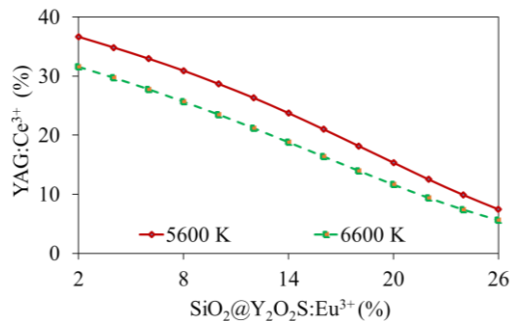


Figure 4. The adjustment of phosphor concentration for retaining the mean CCTs

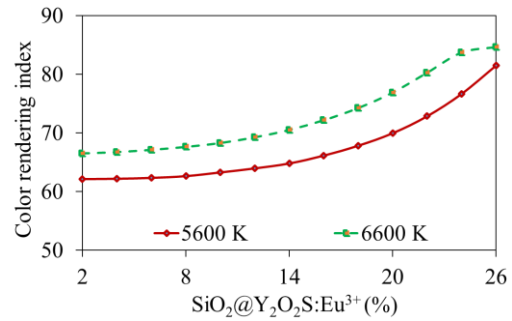


Figure 5. The hue rendering indicator in the WLED device along with YAG:Ce³⁺ content

The PL in the silica-coated  $Y_2O_2S:Eu^{3+}$  ( $SiO_2@Y_2O_2S:Eu^{3+}$ ) was analyzed and displayed in Figure 7. The PL strength of the uncovered and covered  $Y_2O_2S:Eu^{3+}$  phosphors stayed at about 627 nm. This implied that the phosphors yielded red emission in the visible wavelength. Besides that, the in the case of  $SiO_2@Y_2O_2S:Eu^{3+}$  fabricated using P<sub>1</sub> and P<sub>2</sub> methods, the luminous intensity declined slightly. Meanwhile, the phosphors coated with P<sub>3</sub> and P<sub>4</sub> methods showed an improvement in lumen output. For P<sub>1</sub> and P<sub>2</sub> methods, the surface coatings of the phosphor particles are inhomogeneous, which could lead to the decrease in luminous output. In the case of P<sub>3</sub> and P<sub>4</sub> methods, the enhancement in PL intensity can be explained with the following reasons. First, the transparency of the organic and inorganic nanocomposites is generally greater than that of the inorganic xerogel. Second, the refractive index (RI) of PMMA (1.49) is nearly equal to the RI of the silica (1.46), thus minimizing the difference in RI at the coating surface of the phosphors, reducing the light scattering, and enhancing the luminous flux [25], [26]. The matching RI of PMMA-silica also makes the PMMA-silica nano composite coating more transparent than the coating of only silica nanoparticles. In addition to that, PMMA-silica nanocomposite coating contributed greatly to the diffraction and multiplication of visible lights emitted from the phosphors, which probably boost the luminous intensity of the coated phosphors.

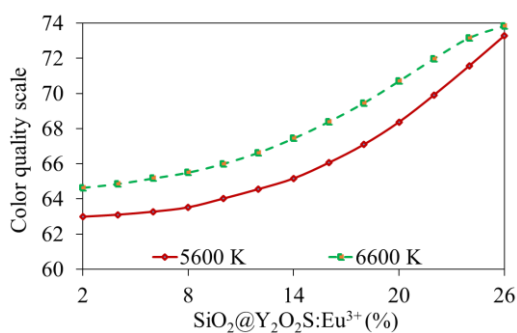


Figure 6. The hue quality scale in the WLED device along with YAG:Ce³⁺ content

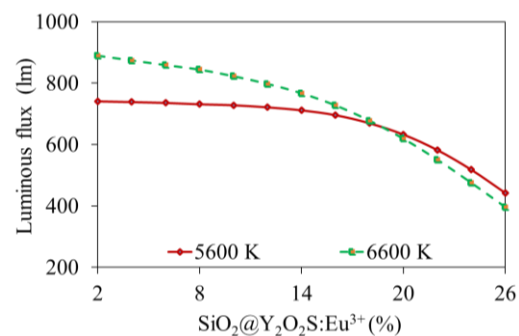


Figure 7. The illuminating beam in the WLED device along with YAG:Ce³⁺ content

The effectiveness of using PMMA-silica nanocomposite surface coating to protect the phosphors from being damaged by environmental factors were verified via CL aging examination. The accelerated aging testing with an electron beam was a 30-minute procedure carried out at a 10-kV acceleration voltage and a  $45 \mu\text{A}/\text{cm}^2$  average current density. The normalized CL intensity for the phosphors with and without surface coatings, under the cumulated aging time. The the phosphors' CL intensity without surface coating dropped as the bombardment period rose, but the CL intensity of the phosphor coated using technique P<sub>4</sub> remained stable. The examination of stability and resistance against the heat and moisture were carried out for both non-coated and coated red phosphors to further investigate the advantages of the surface coating method. These two experiments were carried out by aging the phosphors in a heat-controlled moisture room with a heat of 100 °C and a moisture level of 80%. The results demonstrated that stability of the uncoated phosphor was reduced when being exposed to the heat and moisture. Meanwhile, the PMMA-SiO<sub>2</sub>-nanocomposite coated phosphors (applying P<sub>4</sub> coating method) showed a great stability under heat and moisture during the aging time. Therefore, it can be concluded that the nanocomposite of PMMA and silica nanoparticles is suitable for the surface coating to prevent the irradiation and atmospheric components damaging the phosphor materials.

#### 4. CONCLUSION

In this study, we used four different ways to coat the surface of phosphor Y<sub>2</sub>O<sub>2</sub>S:Eu<sup>3+</sup> accompanied by silica nano-granules as well as PMMA-silica nanocomposite to improve the light output and stability under environmental circumstances of the red phosphor Y<sub>2</sub>O<sub>2</sub>S:Eu<sup>3+</sup>. The phosphor surface coating was carried out on 5 nm nearly mono-disperse SiO<sub>2</sub> nanoparticles. The addition of VP monomer accompanied with a proper content of AIBN initiator into the reaction mixture could prevent the aggregate formation when the primary particle size of silica nanoparticles decreased to 5 nm. The phosphor silica coating on the phosphor surface using the methods of dip coating or sol-gel was inhomogeneous and led to a small decline in PL strength. Meanwhile, the phosphor coating with PMMA-silica nanocomposite was uniform and continuous and subsequently the increase in luminous intensity was observed. In addition to that, PMMA-silica nanocomposite coating using P<sub>4</sub> method enhanced the luminous intensity by 5%, compared to the phosphor without surface coatings. Moreover, the PMMA-silica nanocomposite is suitable to be used as the protective layer. It can enhance the long-term stability of the phosphor because of the effectively protection the phosphor from the negative impacts of irradiation and atmospheric components.

#### ACKNOWLEDGEMENTS

This study was financially supported by Van Lang University, Vietnam.

#### REFERENCES




- [1] T. D. Rubeis, F. Smarra, N. Gentile, A. D'innocenzo, D. Ambrosini, and D. Paoletti, "Learning lighting models for optimal control of lighting system via experimental and numerical approach," *Science and Technology for the Built Environment*, vol.27, no. 8, pp. 1018-1030, Nov. 2021, doi: 10.1080/23744731.2020.1846427.
- [2] N. Eisazadeh, K. Allacker, and F. D. Troyer, "Integrated energy, daylighting and visual comfort analysis of window systems in patient rooms," *Science and Technology for the Built Environment*, vol. 27, no. 8, pp. 1040-1055, Apr. 2021, doi: 10.1080/23744731.2021.1912512.
- [3] J. Zhang, Y. Meuret, X. Wang, and K. A. G. Smet, "Improved and robust spectral reflectance estimation," *Leukos*, vol. 17, no. 3, pp. 359-379, Sep. 2021, doi: 10.1080/15502724.2020.1798246.
- [4] A. M. Salim, and S. A. Dabous, "Quantitative analysis of sustainable housing energy systems based on Estidama pearl rating system," *International Journal of Green Energy*, vol. 15, no. 14-15, Oct. 2018, doi: 10.1080/15435075.2018.1529585.
- [5] K. R. Shailesh, "Understanding multi-domain compact modeling of light-emitting diodes," *Cogent Engineering*, vol. 8, no. 1, Apr. 2021, doi: 10.1080/23311916.2021.1915730.
- [6] M. Y. Mehr, A. Bahrami, W. D. V. Driel, X. J. Fan, J. L. Davis, and G. Q. Zhang, "Degradation of optical materials in solid-state lighting systems," *International Materials Reviews*, vol. 65, no. 2, pp. 102-128, Jan. 2019, doi: 10.1080/09506608.2019.1565716.
- [7] A. Dawodu, A. Cheshmehzangi, and A. Sharifi, "A multi-dimensional energy-based analysis of neighbourhood sustainability assessment tools: are institutional indicators really missing?," *Building Research & Information*, vol. 49, no. 5, pp. 574-592, Sep. 2020, doi: 10.1080/09613218.2020.1806701.
- [8] L. F. Desideri, F. Barra, S. Ferrero, C. E. Traverso, and M. Nicolò, "Clinical efficacy and safety of ranibizumab in the treatment of wet age-related macular degeneration," *Expert Opinion on Biological Therapy*, vol. 19, no. 8, 2019, doi: 10.1080/14712598.2019.1627322.
- [9] S. J. Roberts, J. R. Rudd, and M. J. Reeves, "Efficacy of using non-linear pedagogy to support attacking players' individual learning objectives in elite-youth football: A randomised cross-over trial," *Journal of Sports Sciences*, vol. 38, no. 11-12, pp. 1454-1464, Jun. 2020, doi: 10.1080/02640414.2019.1609894.
- [10] G. Wang, S. C. Hwang, W. H. Kim, and G. S. Kil, "Design and fabrication of an LED lantern based on light condensing technology," *Journal of International Council on Electrical Engineering*, vol. 8, no. 1, pp. 14-18, Jan. 2018, doi: 10.1080/22348972.2018.1436894.
- [11] G. Varan, S. Akkin, N. Demirtürk, J. M. Benito, and E. Bilensoy, "Erlotinib entrapped in cholesterol-depleting cyclodextrin nanoparticles shows improved antitumoral efficacy in 3D spheroid tumors of the lung and the liver," *Journal of Drug Targeting*, vol. 29, no. 4, pp. 439-453, Apr. 2021, doi: 10.1080/1061186X.2020.1853743.






- [12] J. H. Lee *et al.*, "Porous cellulose paper as a light out coupling medium for organic light-emitting diodes," *Journal of Information Display*, vol. 19, no. 4, pp. 171-177, Oct. 2018, doi: 10.1080/15980316.2018.1527260.
- [13] S. C. N. Danny, S. K. F. Nicholas, L. T. Y. Fanny, and Y. Y. L. Timothy, "Ranibizumab for myopic choroidal neovascularization," *Expert Opinion on Biological Therapy*, vol. 20, no. 12, pp. 1385-1393, Dec. 2020, doi: 10.1080/14712598.2021.1830969.
- [14] R. Guerreiro, I. Carpinteiro, L. Proença, M. Polido, and A. Azula, "Influence of acid etching on internal bleaching with 16% carbamide peroxide," *Annals of Medicine*, vol. 53, no. 1, pp. S48-S49, Sep. 2021, doi: 10.1080/07853890.2021.1897351.
- [15] A. Vagge, L. F. Desideri, C. D. Noce, I. D. Mola, D. Sindaco, and C. E. Traverso, "Blue light filtering ophthalmic lenses: A systematic review," *Seminars in Ophthalmology*, vol. 36, no. 7, pp. 541-548, Oct. 2021, doi: 10.1080/08820538.2021.1900283.
- [16] S. Kadyan, S. Singh, S. Sheoran, A. Samantilleke, B. Mari, and D. Singh, "Synthesis and optoelectronic characteristics of MGdAl3O7:Eu3+ nanophosphors for current display devices," *Transactions of the Indian Ceramic Society*, vol. 78, no. 4, pp. 219-226, Dec. 2019, doi: 10.1080/0371750X.2019.1690583.
- [17] S. Sheoran, S. Singh, V. Tanwar, B. M. Soucase, and D. Singh, "Synthesis and optoelectronic characterization of silicate lattice-based M3La2Si3O12 (M = Mg2+, Ca2+, Sr2+ and Ba2+) nanophosphors for display applications," *Transactions of the Indian Ceramic Society*, vol. 79, no. 1, pp. 35-42, Apr. 2020, doi: 10.1080/0371750X.2020.1712259.
- [18] E. Bowditch, E. Chu, and T. Hong, and A. Chang, "Treat and extend paradigm in management of neovascular age-related macular degeneration: current practice and future directions," *Expert Review of Ophthalmology*, vol. 16, no. 4, pp. 267-286, Jun. 2021, doi: 10.1080/17469899.2021.1933439.
- [19] J. Santiago, and P. Sanmartín, "Exposure to artificial daylight or UV irradiation (A, B or C) prior to chemical cleaning: an effective combination for removing phototrophs from granite," *Biofouling*, vol. 34, no. 8, pp. 851-869, Sep. 2018, doi: 10.1080/08927014.2018.1512103.
- [20] L. M. Negi, S. Talegaonkar, M. Jaggi, and A. K. Verma, "Hyaluronate imatinib liposomes with hybrid approach to target CD44 and P-gp overexpressing MDR cancer: an in-vitro, in-vivo and mechanistic investigation," *Journal of Drug Targeting*, vol. 27, no. 2, pp. 183-192, Feb. 2019, doi: 10.1080/1061186X.2018.1497039.
- [21] M. Alavi, and M. Rai, "Recent advances in antibacterial applications of metal nanoparticles (MNPs) and metal nanocomposites (MNCs) against multidrug-resistant (MDR) bacteria," *Expert Review of Anti-infective Therapy*, vol. 17, no. 6, pp. 419-428, Jun. 2019, doi: 10.1080/14787210.2019.1614914.
- [22] A. C. F. A. Vendette, H. L. Piva, L. A. Muehlmann, D. A. D. Souza, A. C. Tedesco, and R. B. Azevedo, "Clinical treatment of intra-epithelia cervical neoplasia with photodynamic therapy," *International Journal of Hyperthermia*, vol. 37, no. 3, pp. 50-58, Dec. 2020, doi: 10.1080/02656736.2020.1804077.
- [23] M. Talone, and G. Zibordi, "Spatial uniformity of the spectral radiance by white LED-based flat-fields," *OSA Continuum*, vol. 3, no. 9, pp. 2501-2511, Sep. 2020, doi: 10.1364/OSAC.394805.
- [24] W. Zhong, J. Liu, D. Hua, S. Guo, K. Yan, and C. Zhang, "White LED light source radar system for multi-wavelength remote sensing measurement of atmospheric aerosols," *Applied Optics*, vol. 58, no. 31, pp. 8542-8548, Nov. 2019, doi: 10.1364/AO.58.008542.
- [25] Z. Zhao, H. Zhang, S. Liu, and X. Wang, "Effective freeform TIR lens designed for LEDs with high angular color uniformity," *Applied Optics*, vol. 57, no. 15, pp. 4216-4221, May 2018, doi: 10.1364/AO.57.004216.
- [26] J. O. Kim, H. S. Jo, and U. Ryu, "Improving CRI and scotopic-to-photopic ratio simultaneously by spectral combinations of CCT-tunable LED lighting composed of multi-chip LEDs," *Current Optics and Photonics*, vol. 4, no. 3, pp. 247-252, Jun. 2020, doi: 10.1364/COPP.4.000247.

## BIOGRAPHIES OF AUTHORS



**Van Liem Bui**    received a Bachelor of Mathematical Analysis and master's in mathematical Optimization, Ho Chi Minh City University of Natural Sciences, VietNam. Currently, He is a lecturer at the Faculty of Fundamental Science, Industrial University of Ho Chi Minh City, Viet Nam. His research interests are Mathematical Physics. He can be contacted at email: buivanliem@iuh.edu.vn.



**Phan Xuan Le**    received a Ph.D. in Mechanical and Electrical Engineering from Kunming University of Science and Technology, Kunming city, Yunnan province, China. Currently, He is a lecturer at the Faculty of Engineering, Van Lang University, Ho Chi Minh City, Viet Nam. His research interests are Optoelectronics (LED), Power transmission and Automation equipment. He can be contacted at email: le.px@vlu.edu.vn.